

A parabolic notch interacting with a generalized anti-plane singularity

Lifeng Ma^{1,2*}, Yifeng Chen³, David A. Hills^{3*}

1. Department of Mechanical, Materials and Manufacturing Engineering, University of Nottingham, University Park, NG7 2RD, UK.
2. S&V Lab, Department of Engineering Mechanics, Xi'an Jiaotong University, 710049 Xi'an, China
3. Department of Engineering Science, Oxford University, OX1 3PJ, Oxford, UK

Abstract

In this study, the interaction of a parabolic notch with a generalized anti-plane singularity is studied and its analytical solution is derived. The singularity may be either an anti-plane concentrated force or a screw dislocation, and separate solutions for each of these are found. The driving force present on the screw dislocation due to the notch free boundary is obtained. It is found that a dislocation-free zone may exist beneath the notch root surface when the screw dislocation is placed on the notch geometric symmetry axis, as the driving force will pull dislocations to the free boundary where they will be annihilated. The solutions developed in this study may be used as building blocks to model the damage of material near a parabolic notch under anti-plane load conditions, and therefore serve as a step in quantifying crack nucleation conditions, which is the novelty of the current study.

Keywords: Singularity, parabolic notch, screw dislocation, anti-plane concentrated force, conformal mapping.

1. Introduction

* Corresponding authors

Email addresses: malf@mail.xjtu.edu.cn (L. Ma); David.Hills@eng.ox.ac.uk (D. A. Hills)

A notch is a common feature necessarily figuring in many mechanical components, possibly included for practical requirements such as component assembly (the grooves needed for retention clips, for example) or power transmission, as in the shaft spline. A knowledge of the stress fields ahead of notches is essential during design and fatigue assessment. To understand the stress distribution near notches, great efforts have been put into studying this topic. There are two fundamental classes: ‘sharp’ and ‘blunt’.

Considering the sharp notch first and also ‘in-plane’ loading, Williams [1] developed a method for expanding the Airy stress function as an eigenfunction series, presenting an asymptotic solution for the distribution of stress around a sharp V-notch. Traditional notch stress intensity factors are the multipliers on first symmetric and anti-symmetric terms in Williams’ solution. The factors can be thought of as the extensions of the conventional stress intensity factors used for cracked components. But, the most important property of the solution found is that the eigensolutions provide very precise information about stress gradients and the spatial distribution of stresses; they therefore provide a lot of information about the neighbourhood in which cracks may potentially start, and it is straightforward to represent the environment present in a complicated prototype in a laboratory experiment to a very high degree of fidelity.

Now, turning to *blunt* notches and again ‘in-plane’ loading, Neuber [2] dealt with the stress *concentration* for a blunt notch using the first term in a series expansion of Airy biharmonic potential functions. The simple stress concentration factor was adopted to directly characterize the stress field of blunt notches *at a point* (see, e.g., [3-7]). It seems that this approach is perceived to be simpler in practical engineering so that it has been widely employed (e.g., [8-12]). It is attractive because

of its simplicity, but a lot of information is lost by this approach. In particular, there is no information about the gradients of stress, nor their spatial distribution.

Approaching the problem from the opposite direction, by taking advantage of the Kolosov-Muskhelishvili complex variable formulae [13], the sharp V-notch was investigated with finite representative complex terms by Carpenter [14-17]. And, following Carpenter's efforts, by combining the Kolosov-Muskhelishvili approach with Neuber's conformal mapping [2,13], a substantial attempt to provide a unified approach to the analysis of cracks, sharp and blunt V-notches was proposed by Lazzarin and Tovo [18]. In order to improve the accuracy of the approach and its application, much further work has been done (see, e.g., [19-21]). In these studies notch problems are treated by a stress function series expansion, or by employing a series terms to find asymptotic or approximate solutions.

In addition to the in-plane deformation, notches under anti-plane load or torsion loading have even been received particular attention since the excellent pioneering investigations of stress fields around grooves or cracks [22-25]. Torsion of circular shafts is, of course, a problem in which a surface notch undergoes, locally, pure anti-plane loading. In more general problems notches may experience complicated states of stress which, locally, comprise an in-plane pair of loads (opening and shear) together with an anti-plane contribution.

Within the framework of a geometrically plane assumption, studies of both the sharp V-notch and blunt V-notch under anti-plane loading has been conducted for a long time (see, e.g., [26-32]). The stress distributions near the root of an elliptically cylindrical notch under torsional loading has been documented (see, e.g., [33, 34]). Elastic stress distributions for hyperbolic, parabolic and more generalized notches in round shafts under torsion and uniform anti-plane shear loading have been analyzed

[35, 36]. Recently, a unified solution approach for a large variety of anti-plane shear and torsion notch problems has been performed by Salviato and Zappalorto [37]. The main approaches employed in these studies are either direct approximate elastic solutions, or the complex potential method used in combination with all kinds of transform into curvilinear coordinates (see, e.g., [2]).

The work described above represents very considerable progress in our understanding of the problems but some remaining challenges still exist. Firstly, strictly speaking, the aforementioned analysis has been conducted in an asymptotic or approximate sense. It is hard to cover various load conditions, including the far-field loads, and the near-field loads such as acting body force loads and displacement loads in the neighborhood of notches. Secondly, apart from some finite element simulations, the damage such as crack initiation, crack propagation, or plastic deformation, occurred near the root of notches due to high stress concentration, can be modelled in terms of continuous dislocation distribution through Green's function method, which is able to reflect the physical damage mechanism. However, at present, its kernel function is hard to be established. These challenges demand a rigorous and thorough analysis on the blunt notch problems. As a first step, in this paper the parabolic notch is studied, and the effect of generalized singularity, producing an anti-plane stress field in its neighbourhood, is found. This complements our recent efforts in establishing the corresponding solution for in-plane loading [38].

The aim of this complementary study is to develop a fundamental solution for a parabolic notch interacting with a generalized anti-plane singularity. The singularity may be either an out-of-plane concentrated force or a screw dislocation, or various combinations of them, which may lead to a moment load, a residual stress (or strain) state, and so on (see, e.g., [39]). The intended application of the results is two-fold;

first, as a means of generating a wide range of equivalent remote loads in a simple and versatile way, and secondly, to provide the possibility of analyzing local notch root plasticity in a way which correctly tracks out the plastic flow rules.

Following this strategy, we use complex variable methods to derive closed-form solutions to the problem of a parabolic notch interacting with the anti-plane singularity. The basic geometry we will consider is shown in Fig. 1, in which, the generalized anti-plane singularity is arbitrarily located within the infinite notched solid.

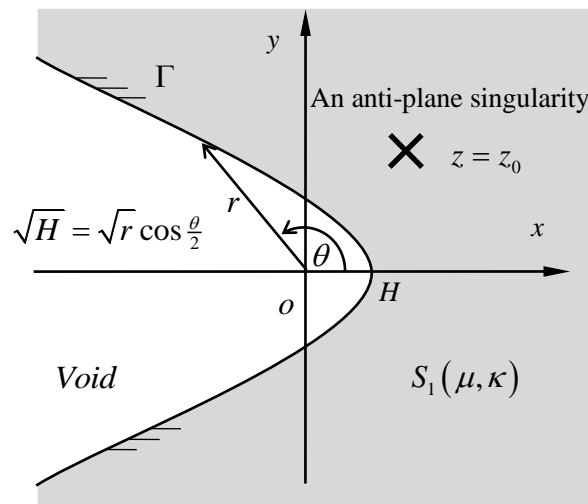


Fig. 1 The configuration of a parabolic notch interacting with a generalized anti-plane singularity which is located at an arbitrary point within solid S_1 , and the void is

located at the left side.

The procedure followed is outlined as follows: first, the complex formulae for anti-plane deformation and the generalized anti-plane singularity are presented in §2, and the basic model is formulated in §3. The solution for the interaction between a parabolic notch and an anti-plane singularity is derived in §4. Subsequently, in §5, two examples are analyzed: first a parabolic notch interacting with a pair of concentrated forces, and secondly a parabolic notch interacting with a screw

dislocation. The force present on the dislocation is derived. Finally conclusions are drawn in §6.

2. The complex framework and its form for a generalized anti-plane singularity

In this section, complex variable formulae for out-of-plane problems and boundary conditions are introduced. The general singularity model is introduced which provides a basic concept for subsequent analysis.

2.1 The complex potential formulae

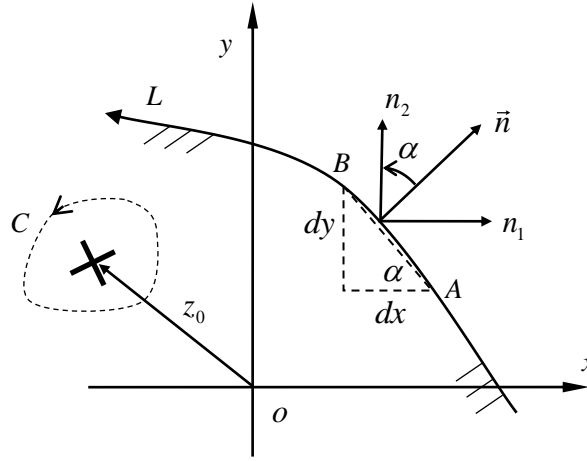


Fig. 2 The framework of anti-plane deformation and a generalized anti-plane singularity (shown here by a cross sign) embedded within a plane solid whose boundary is L .

In the anti-plane shear deformation of an isotropic elastic material, the in-plane displacements are $u = v = 0$, and the out-of-plane displacement is $w = w(x, y)$. The geometric equations, the constitutive equation and the equilibrium equation are as follows

$$\gamma_{13} = \frac{\partial w}{\partial x}, \gamma_{23} = \frac{\partial w}{\partial y}, \sigma_{13} = \mu \gamma_{13}, \sigma_{23} = \mu \gamma_{23}, \frac{\partial \sigma_{13}}{\partial x} + \frac{\partial \sigma_{23}}{\partial y} = 0, \quad (1)$$

where γ_{13} and γ_{23} are strains, σ_{13} and σ_{23} are anti-plane shear stresses, and μ is the shear modulus. From Eq. (1) we get

$$\frac{\partial^2 w}{\partial^2 x} + \frac{\partial^2 w}{\partial^2 y} = 0. \quad (2)$$

Its formal solution can be expressed in terms of a holomorphic function $f(z)$ of the complex variable $z = x_1 + ix_2 (= x + iy)$ as

$$w = -\frac{i}{2} [f(z) - \bar{f}(\bar{z})], \quad (3)$$

where $i = \sqrt{-1}$.

With the help of Eq. (3), the two stress components can be rewritten as

$$\begin{cases} \sigma_{13} = \mu \frac{\partial w}{\partial x} = -\frac{i}{2} \mu [f'(z) - \bar{f}'(\bar{z})] \\ \sigma_{23} = \mu \frac{\partial w}{\partial y} = \frac{\mu}{2} [f'(z) + \bar{f}'(\bar{z})] \end{cases}. \quad (4)$$

Now, we consider traction boundary condition shown in Fig. 2. Let t_3 be the nonzero traction component along the x_3 -direction on a boundary L , with material present on the left-hand side. The resultant traction can be written as:

$$t_3 = \sigma_{i3} n_i = \sigma_{13} n_1 + \sigma_{23} n_2 = \sigma_{13} \frac{\partial y}{\partial s} - \sigma_{23} \frac{\partial x}{\partial s}, \quad (5)$$

where $n_1 = \frac{\partial y}{\partial s}$, $n_2 = -\frac{\partial x}{\partial s}$ are components of the surface unit normal. In consideration of the equilibrium equation in Eq. (1), the two stress components can be related to a stress function ϕ as

$$\sigma_{13} = -\phi_{,2} \quad \sigma_{23} = \phi_{,1}. \quad (6)$$

So Eq. (5) can be reformulated as

$$t_3 = \sigma_{i3} n_i = \sigma_{13} n_1 + \sigma_{23} n_2 = -\phi_{,2} \frac{\partial y}{\partial s} - \phi_{,1} \frac{\partial x}{\partial s} = -\frac{d\phi}{ds}. \quad (7)$$

Alternatively, because

$$\begin{cases} n_1 = \frac{\partial y}{\partial s} = \frac{\partial(z - \bar{z})}{2i\partial s} = \frac{1}{2} \left(-i \frac{\partial z}{\partial s} + i \frac{\partial \bar{z}}{\partial s} \right) \\ n_2 = -\frac{\partial x}{\partial s} = -\frac{\partial(z + \bar{z})}{2\partial s} = -\frac{1}{2} \left(\frac{\partial z}{\partial s} + \frac{\partial \bar{z}}{\partial s} \right) \end{cases}, \quad (8)$$

Eq. (5) can be rewritten as

$$t_3 = \sigma_{i3} n_i = \sigma_{13} n_1 + \sigma_{23} n_2 = -\frac{\mu}{2} \frac{\partial [f(z) + \bar{f}(\bar{z})]}{\partial s}. \quad (9)$$

Thus by combining Eqs. (7) and (9), we have

$$t_3 = -\frac{\mu}{2} \frac{\partial [f(z) + \bar{f}(\bar{z})]}{\partial s} = -\frac{\partial \phi}{\partial s}. \quad (10)$$

The resultant force acting on an arc AB is (see, Fig. 2)

$$T_3 = \int_A^B t_3 ds = -\frac{\mu}{2} [f(z) + \bar{f}(\bar{z})] \Big|_A^B = -\phi \Big|_A^B. \quad (11)$$

Furthermore, using the above formulae, we can obtain

$$\begin{cases} \sigma_{23} + i\sigma_{13} = \mu f'(z) \\ \phi + i\mu w = \mu f(z) \end{cases}, \quad (12)$$

where the constant is discarded during the operation. Eqs. (11) and (12) will be frequently used in the following manipulation.

2.2 The complex potential for singularities

A generalized anti-plane singularity, located at z_0 in an infinite plane, which may be a screw dislocation or an anti-plane concentrated force, has a complex variable potential which may be expressed as

$$f_0(z) = A \ln(z - z_0), \quad (13)$$

where A is a complex number, to be determined by one of the following singularity conditions

$$\begin{cases} b_z = \oint_{\gamma_0} dw \\ F_z = -\oint_{\gamma_0} dT_3 = \oint_{\gamma_0} d\phi \end{cases} \quad (14)$$

The contour of integration should enclose the singularity z_0 , and in the first equation b_z is the Burgers vector while in the second F_z is the out-of-plane concentrated force in z - direction. Inserting Eq. (13) into the last equation in Eq. (12), and considering Eq. (14), we obtain

$$f_0(z) = \frac{(F_z + i\mu b_z)}{2\pi\mu i} \ln(z - z_0). \quad (15)$$

If $F_z = 0$, it degenerates to the complex variable potential for a screw dislocation in infinite solid:

$$f_0(z) = \frac{b_z}{2\pi} \ln(z - z_0), \quad (16)$$

while if $b_z = 0$, it degenerates to the solution for an out-of-plane concentrated force as

$$f_0(z) = \frac{F_z}{2\pi\mu i} \ln(z - z_0). \quad (17)$$

With Eq. (15) established, the complex potential for an anti-plane concentrated moment or an anti-plane eigenstrain nucleus may also be derived (see e.g., [39-41]).

3. Formulation

3.1 Physical problem

Consider a parabolic notch with a surface Γ which extends to infinity, as shown in Fig. 1, where a generalized anti-plane singularity is located in the substrate material. The parabolic surface can be described by the following function in a polar coordinate set, as set out by [35]

$$h = \sqrt{H} = \sqrt{r} \cos \frac{\theta}{2}, \quad (18)$$

where h and H are constant numbers, and H has a length dimension. Its corresponding expression in rectangular coordinate system is

$$x = H - \frac{y^2}{4H}, \quad \text{or} \quad \left(\frac{x}{H} \right) = 1 - \frac{1}{4} \left(\frac{y}{H} \right)^2. \quad (19)$$

This implies that a series of parabolic notches can be described in a standard expression.

For this geometry, the complex potentials within the elastic solid, identified as S_1 can be constructed from

$$f(z) = f_0(z) + f_1(z), \quad z \in S_1, \quad (20)$$

where $f_0(z)$ represents the complex potential of a generalized anti-plane singularity in an infinite plane shown in Eq. (15), and $f_1(z)$ is a regular perturbed complex potential in S_1 , which will be determined from the free surface boundary condition. It should be pointed out that $f_1(z)$ will reflect the material presence, the geometric surface boundary conditions, and incorporate the presence of the singularity.

3.2 Conformal mapping

To solve the physical problem, it is convenient to map the physical configuration onto an auxiliary configuration in which the surface is mapped into a straight line, so that the traditional complex variable techniques can be employed to solve the problem. To this end we introduce the mapping function as follows

$$\begin{cases} z = x + iy = re^{i\theta} = \omega(\zeta) = (-i\zeta + h)^2, h > 0 \\ \zeta = \omega^{-1}(z) = i\left(z^{\frac{1}{2}} - h\right) = u + iv, h = \sqrt{H} \end{cases}. \quad (21)$$

We find that

$$v = \sqrt{r} \cos \frac{\theta}{2} - h, \quad u = -\sqrt{r} \sin \frac{\theta}{2}. \quad (22)$$

The mapping functions (21) map the physical z -plane in Fig. 3a onto the auxiliary ζ -plane in Fig. 3b. It may be observed from Fig. 3 that the material S_1 in Fig. 3a is mapped onto the upper plane in Fig. 3b, while the void in Fig. 3a is mapped onto the lower plane in Fig. 3b. The free surface is mapped into the u -axis in ζ -plane.

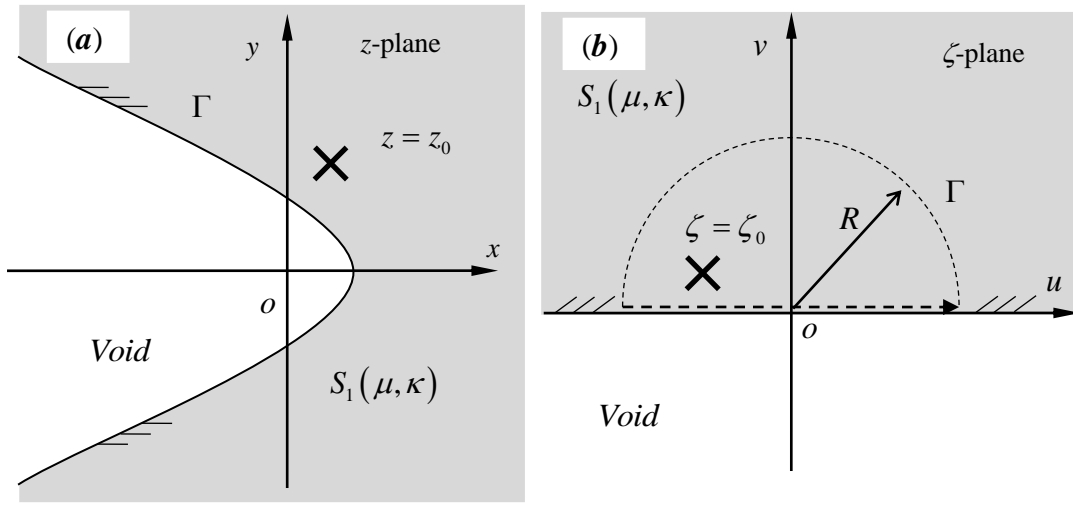


Fig. 3 A parabolic notch in an infinite plane interacting with a singularity located in material S_1 (right-side): (a) physical model, (b) auxiliary plane

In terms of the mapping, Eq. (11) can be rewritten as

$$T_3 = -\frac{\mu}{2} \left[\hat{f}(\zeta) + \overline{\hat{f}(\zeta)} \right], \quad (23)$$

and Eq. (20) will be transformed to

$$\hat{f}(\zeta) = \hat{f}_0(\zeta) + \hat{f}_1(\zeta), \quad \zeta \in S_1, \quad (24)$$

in which, accordingly,

$$\begin{aligned} \hat{f}_0(\zeta) &= f_0(\omega(\zeta)) = A \ln \left((-i\zeta + h)^2 - (-i\zeta_0 + h)^2 \right) \\ &= A \ln(\zeta_0 - \zeta) + A \ln(\zeta + \zeta_0 + 2hi) \end{aligned} \quad (25)$$

According to Liouville's theorem, it is logically assumed that the function $\hat{f}_1(\zeta)$ is regular within S_1 and singular within S_2 , while $\overline{\hat{f}_1}(\zeta)$ is regular within S_2 and singular within S_1 in Fig. 3b.

With the traction-free condition on the notch surface ($\text{Im}(\zeta) = v = 0$) in Fig. 3b, inserting Eq. (24) into Eq. (23) leads to

$$\hat{f}_0(\zeta) + \hat{f}_1(\zeta) + \overline{\hat{f}_0(\zeta)} + \overline{\hat{f}_1(\zeta)} = 0, (\zeta = u). \quad (26)$$

Further, by substituting Eq. (25) into Eq. (26), it can be rearranged to give

$$\begin{aligned} A \ln(\zeta_0 - u) + A \ln(u + \zeta_0 + 2hi) + \hat{f}_1(u) + \bar{A} \ln(\bar{\zeta}_0 - u) \\ + \bar{A} \ln(u + \bar{\zeta}_0 - 2hi) + \overline{\hat{f}_1}(u) = 0 \end{aligned} \quad (27)$$

Eq. (27) is a typical boundary value problem in terms of complex variables with a specific mapping, from which $\hat{f}_1(\zeta)$ is to be determined. Once it is solved, the primitive function $f_1(z)$ in Eq. (20) will be fixed.

4. Solution

In this section, some integral formulae will be presented. By virtue of these identities, Eq. (27) will be solved.

4.1 Integral formulae: Cauchy's integral formula and integral formulae for holomorphic function with singularities

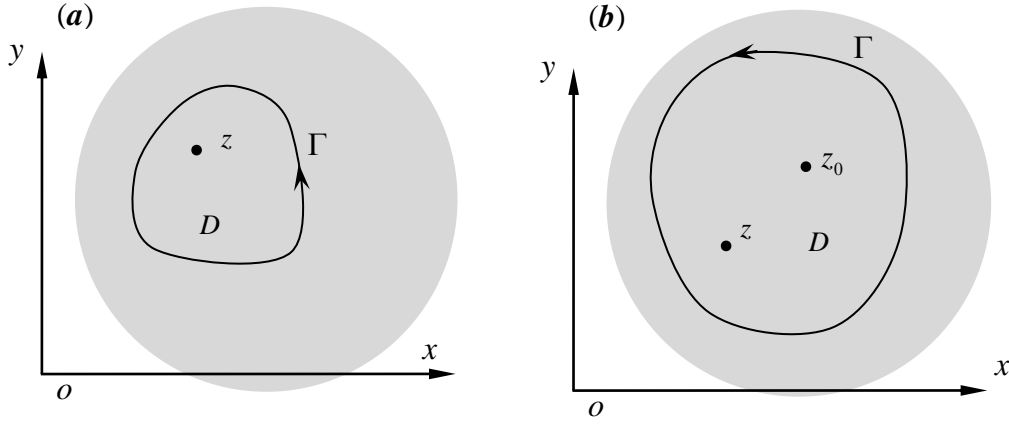


Fig. 4 Integral formulae and function holomorphy in a complex plane: (a) function holomorphy in a domain, (b) function holomorphy in a domain but with a singularity in the integral contour.

Cauchy's integral formula would play a key role in the following manipulation. It can be described as: A holomorphic function $f(z)$ defined on a domain D enclosed by a curve Γ is completely determined by its values on the boundary Γ (see Fig. 4a)

$$f(z) = \begin{cases} \frac{1}{2\pi i} \oint_{\Gamma} \frac{f(t) dt}{(t-z)}, & (z \in D) \\ 0, & (z \notin D) \end{cases}. \quad (28)$$

and it also results in integral formulas for all derivatives of the holomorphic function as

$$f^{(n)}(z) = \begin{cases} \frac{n!}{2\pi i} \oint_{\Gamma} \frac{f(t) dt}{(t-z)^{n+1}}, & (z \in D) \\ 0, & (z \notin D) \end{cases} \quad n \geq 0. \quad (29)$$

On the other hand, if there is a singularity within the holomorphic plane, as shown in Fig. 4b, $\lim_{t \rightarrow z_0} f(t) = \infty$, and the singularity is enclosed within the contour, we can prove that [38]

$$\frac{n!}{2\pi i} \oint_{\Gamma} \frac{f(t)dt}{(t-z)^{n+1}} = \begin{cases} Cf(\infty), (z \in D, n=0) \\ 0, (z \in D, n \geq 1) \end{cases}. \quad (30)$$

where C is a finite constant and $f(\infty)$ is a constant at infinity. For convenience, we suppose that $\lim_{z \rightarrow \infty} f(z) = 0$ which does not influence the stress analysis in this study.

So that

$$\frac{n!}{2\pi i} \oint_{\Gamma} \frac{f(t)dt}{(t-z)^{n+1}} = 0, (z \in D, n \geq 0). \quad (31)$$

4.2 Solution

Because $\hat{f}_0(\zeta)$ and $\bar{\hat{f}}_1(\zeta)$ are non-holomorphic while $\bar{\hat{f}}_0(\zeta)$ and $\hat{f}_1(\zeta)$ are holomorphic within the upper plane in Fig. 3b, multiplying both sides of Eq. (27) by $\frac{1}{2\pi i} \frac{du}{(u-\zeta)}$ and performing the integration along the contour Γ in the upper plane

in Fig. 3b as $R \rightarrow \infty$, and considering Eqs. (29) and (31), we obtain

$$\hat{f}_1(\zeta) + A \ln(\zeta + \zeta_0 + 2hi) + \bar{A} \ln(\bar{\zeta}_0 - \zeta) = 0, \quad (32)$$

which gives

$$\hat{f}_1(\zeta) = -A \ln(\zeta + \zeta_0 + 2hi) - \bar{A} \ln(\bar{\zeta}_0 - \zeta). \quad (33)$$

This is the perturbed potential solution in the auxiliary plane. It can be verified that it is regular in the upper ζ -plane, which completely complies with the preceding assumption.

Now, by substituting $\zeta = i(\sqrt{z} - h)$ from Eq. (21) into Eq. (33), it follows that

$$f_1(z) = -A \ln \left[i(\sqrt{z} + \sqrt{z_0}) \right] - \bar{A} \ln \left[-i(\sqrt{z_0} + \sqrt{z} - 2h) \right]. \quad (34)$$

After discarding the constants involved in the above expression, which do not influence the stress expression in Eq. (12), the solution (20) for the singularity-notch interaction problem is finally seen to be

$$f(z) = f_0(z) + f_1(z) = A \ln(z - z_0) - A \ln(\sqrt{z} + \sqrt{z_0}) - \bar{A} \ln(\sqrt{z_0} + \sqrt{z} - 2h). \quad (35)$$

By inserting the function $f(z)$ into Eq. (12), the stress and displacement fields can be found.

It should be mentioned that the analytic solution for a screw dislocation interacting with a parabolic elastic inhomogeneity has been recently derived by Wang and Schiavone [42]. Their solution was expressed as a complex variable series.

5. Examples: Analytical solution for the parabolic notch interacting with singularities

In §4, we have obtained the general solution. In this section we present two examples, as shown in Fig. 5: (a) a parabolic notch under two opposing concentrated anti-plane forces which are symmetrically distributed along the two sides of symmetric line x -axis, and (b) a parabolic notch interacting with a screw dislocation. The first example is to numerically verify the foregoing equation manipulation. The second is to investigate the configuration-force acting on the screw dislocation. For simplicity, but without loss of the generality, we here set $H = 1$, which would imply that other variables involved such as z , z_0 Burgers vector b_z , and F_z would be simultaneously treated as being divided by H (see Eq. (21), $H = h^2$).

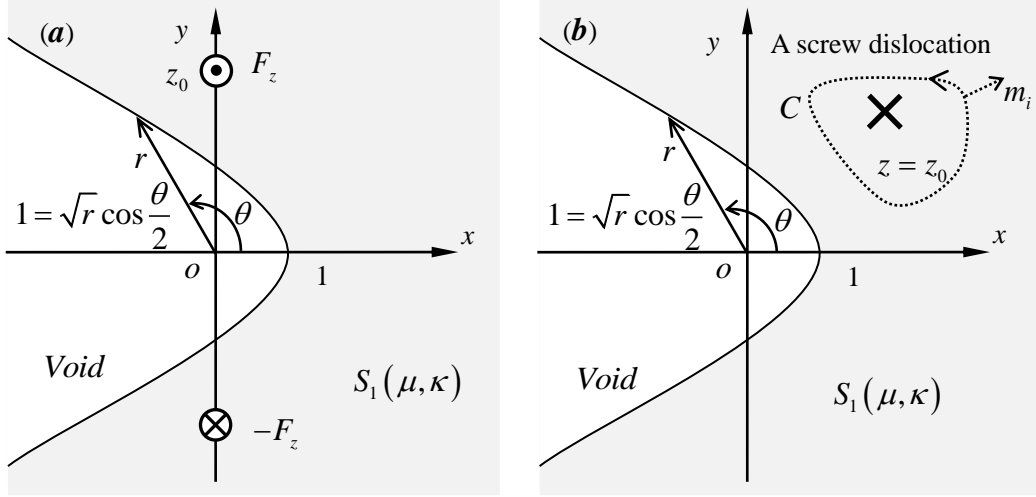


Fig. 5 Examples: (a) a parabolic notch under two opposed concentrated anti-plane forces which are symmetrically distributed along the two side of symmetric line x -axis; (b) a parabolic notch interacting with a screw dislocation.

5.1 Stress field excited by the two concentrated forces (see Fig. 5a)

Since there are two singularities which are symmetrically distributed as shown in Fig. 5a, the complex potential solution for the problem can be assembled as

$$f(z) = \frac{F_z}{2\pi\mu i} \left[\ln(z - z_0) - \ln(\sqrt{z} + \sqrt{z_0}) + \ln(\sqrt{z_0} + \sqrt{z} - 2) \right] - \frac{F_z}{2\pi\mu i} \left[\ln(z - \bar{z}_0) - \ln(\sqrt{z} + \sqrt{\bar{z}_0}) + \ln(\sqrt{z_0} + \sqrt{z} - 2) \right] \quad (36)$$

and its derivative is

$$f'(z) = \frac{F_z}{2\pi\mu i} \left[\frac{1}{(z - z_0)} - \frac{1}{(z - \bar{z}_0)} + \frac{1}{2\sqrt{z}(\sqrt{z} + \sqrt{\bar{z}_0})} - \frac{1}{2\sqrt{z}(\sqrt{z} + \sqrt{z_0})} + \frac{1}{2\sqrt{z}(\sqrt{\bar{z}_0} + \sqrt{z} - 2)} - \frac{1}{2\sqrt{z}(\sqrt{z_0} + \sqrt{z} - 2)} \right]. \quad (37)$$

Inserting Eq. (37) into the first equation of Eq. (12), the stress field will be immediately derived. To provide an illustration of the stress distribution, we take $z_0 = 6i$ in Fig. 5a. The stress distributions induced are plotted in Fig. 6, in which the

normalized stresses are defined as $\bar{\sigma}_{i3} = 2\pi\sigma_{i3}/F_z$. It can be observed from Fig. 6 that:

(i) the stress $\bar{\sigma}_{13}$ is anti-symmetrically distributed about x -axis so that its value is always 0 along the x -axis; (ii) the stress $\bar{\sigma}_{23}$ is symmetrically distributed about x -axis and the stress is concentrated around the notch throat. These stress distribution patterns partially demonstrate the reliability of the above solutions we derived.

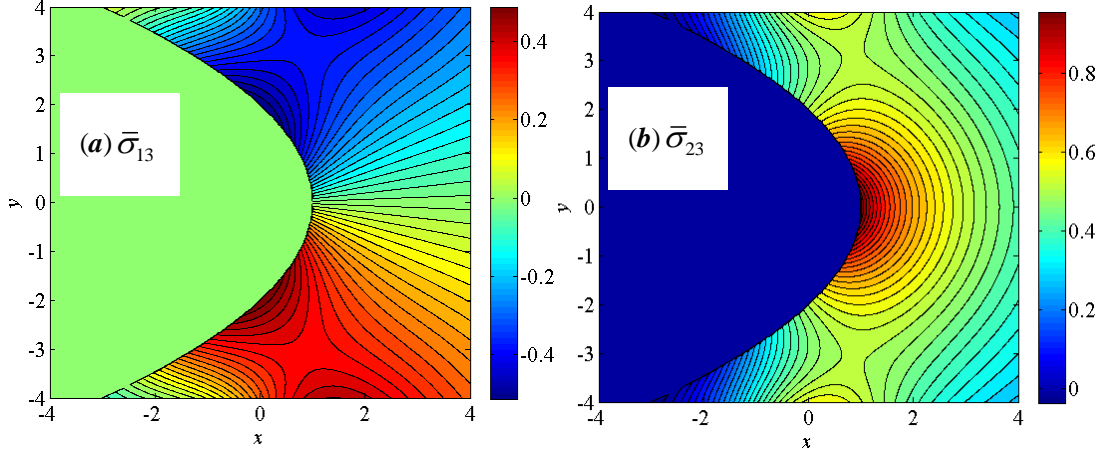


Fig. 6 Normalized stress distribution at the notch throat due to two opposite concentrated anti-plane forces respectively acting at the points (0,6) and (0,-6);

$$(a) \quad \bar{\sigma}_{13} = 2\pi\sigma_{13}/F_z, \quad (b) \quad \bar{\sigma}_{23} = 2\pi\sigma_{23}/F_z$$

5.2 The driving force on the dislocation (see Fig. 5b)

As shown in Fig. 5b, a screw dislocation is embedded within the substrate and the complex potential solution for this problem will be

$$f(z) = f_0(z) + f_1(z) = A \ln(z - z_0) - A \ln(\sqrt{z} + \sqrt{z_0}) - \bar{A} \ln(\sqrt{\bar{z}_0} + \sqrt{z} - 2) \quad (38)$$

where $A = b_z/2\pi$ and the Burgers vector b_z should be understood by being normalized by H as before.

The presence of a curved free surface or an external force causes a force to act on the singularity, and this may be evaluated through the vector integral J_i , which was originally introduced by Eshelby [43], and later on its component $J = J_1$ was

independently introduced into fracture mechanics by Cherepanov [44] and Rice [45].

The integrals J_1 and J_2 can be written as:

$$J_i = \oint_C \left(w m_i - T_j \frac{\partial u_j}{\partial x_i} \right) ds = \oint_C \left(w m_i - T_3 \frac{\partial w}{\partial x_i} \right) ds, \quad (i=1,2) \quad (39)$$

where m_i is the vector normal to the integral path C in Fig. 5b, T_3 are the resultant forces acting on integral path and w are displacement on it in anti-plane direction, the strain energy density can be expressed as $w = \int_0^{\varepsilon_{ij}} \sigma_{ij} d\varepsilon_{ij}$. It should be pointed out that (i) both J_1 and J_2 are path-independent integrals, i.e. each integral has an identical value for any integral path enclosing the singularity, and (ii) J_1 and J_2 are the components of the driving force acting on the singularity in x -direction and y -direction, respectively.

Alternatively, the combination of the two integrals can be expressed in terms of the complex potential as [46]

$$J_1 - iJ_2 = -\frac{\mu i}{2} \oint_C [f'(z)]^2 dz. \quad (40)$$

By substituting Eq. (38) into Eq. (40), the driving force is found to be

$$\begin{aligned} J_1 - iJ_2 &= -\frac{\mu i}{2} \oint_C \left[\frac{A}{(z - z_0)} - \frac{A}{2\sqrt{z}(\sqrt{z} + \sqrt{z_0})} - \frac{\bar{A}}{2\sqrt{z}(\sqrt{z_0} + \sqrt{z} - 2)} \right]^2 dz \\ &= -\mu\pi \left[\frac{A^2}{2z_0} + \frac{A\bar{A}}{\sqrt{z_0}(\sqrt{z_0} + \sqrt{z_0} - 2)} \right] \end{aligned} \quad (41)$$

If we write $z_0 = re^{i\alpha}$, the expressions for J_1 and J_2 can be separately written as

$$\begin{cases} J_1 = -\frac{\pi\mu A^2}{2} \left(\frac{\cos \alpha}{r} + \frac{2\cos \psi}{R} \right) \\ J_2 = -\frac{\pi\mu A^2}{2} \left(\frac{\sin \alpha}{r} + \frac{2\sin \psi}{R} \right) \end{cases}, \quad (42)$$

where

$$\begin{cases} R = \left[\left(r + r \cos \alpha - 2\sqrt{r} \cos \frac{\alpha}{2} \right)^2 + \left(r \sin \alpha - 2\sqrt{r} \sin \frac{\alpha}{2} \right)^2 \right]^{\frac{1}{2}} \\ \tan \psi = \frac{\left(r \sin \alpha - 2\sqrt{r} \sin \frac{\alpha}{2} \right)}{\left(r + r \cos \alpha - 2\sqrt{r} \cos \frac{\alpha}{2} \right)} \end{cases}. \quad (43)$$

It can be found from Eqs. (42) and (43) that, if $-\delta \leq \alpha \leq \delta$, where δ is a small positive number, $J_1 < 0$, and the direction of J_2 is always pointing to the geometric symmetric line x -axis.

If the dislocation is exactly located on the x -axis and no external force applied, we also find that $J_2 = 0$, and the normalized J_1 becomes

$$\bar{J}_1 = \frac{2}{\mu\pi A^2} J_1 = -\left(\frac{1}{x} + \frac{1}{\sqrt{x}-1} - \frac{1}{\sqrt{x}} \right). \quad (44)$$

By using Eq. (44), the driving force J_1 on the screw dislocation versus its location on x -axis in Fig. 5b is drawn and shown in Fig. 7.

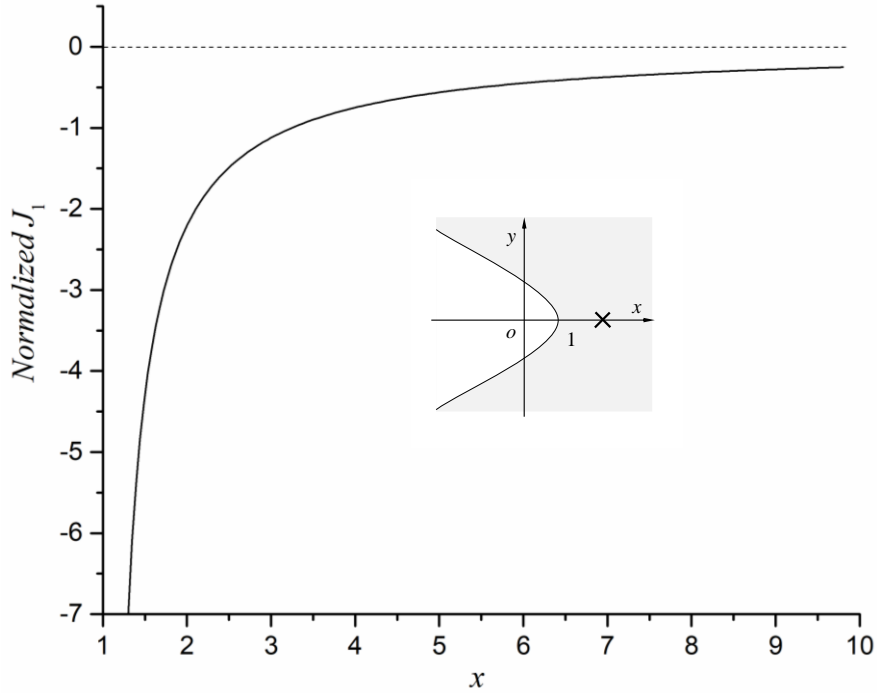


Fig. 7 The driving force J_1 on the screw dislocation versus its location along x -axis

(The inset is the physical configuration of notch showing the screw dislocation position.)

It is observed from Fig. 7 that the driving force on the screw dislocation resulting just from the presence of the free boundary has a drastic variation with x . It is a persistent force that tends to drive the dislocation out of the substrate towards the free surface. When the dislocation is located near the surface, the driving force will be large enough to overcome the material internal resistance to impel it out of the substrate, which may result a dislocation-free area. However, when the dislocation is located deeply inside of the substrate, the driving force on the dislocation rapidly decreases, and it may be verified that when $x \rightarrow \infty$ in Eq. (44), the driving force $J_1 \rightarrow 0$.

The two examples we considered in this section are just the simplest scenarios of the parabolic notch interacting with singularities, but they may be regarded as tests to verify the derivation of the general solution, and at the same time, they may shed some light on the mechanism of notch-singularity interaction.

6. Concluding remarks

In this study, using the complex conformal mapping technique, the analytical solution for a parabolic notch in a plane infinite solid, interacting with a generalized anti-plane singularity has been derived. The singularity may be thought of as representing either a screw dislocation or a concentrated anti-plane force. To demonstrate its application and verify its correctness, a parabolic notch separately interacting with concentrated forces and a screw edge dislocation have been investigated in detail. The driving force on the screw dislocation has been obtained, from which the dislocation-free zone can be predicted.

The solutions developed can be used as building blocks to model the parabolic notch damage problems such as crack initiation and propagation, with the distributed dislocation technique [47], and the parabolic notch under complex load conditions simulated with Green's function method. Moreover, the approach developed in this study may be also used to solve further hyperbolic notch-singularity interaction problems. These are the evident novelties of the current study in comparison with the results in literature.

Acknowledgements

The support of the Sir Joseph Pope Fellowship from Nottingham University is much appreciated. This work was also partially supported by National Natural Science Foundation of China (grant nos. 12072254 and 41630634).

References

- [1] Williams, M.L., 1952, "Stress singularities resulting from various boundary conditions in angular corners of plates in extension," J. Appl. Mech., **19**, pp. 526-528.
- [2] Neuber H., 1958, Theory of Notch Stresses: Principles for Exact Calculation of Strength with Reference to Structural Form and Material. Berlin: Springer-Verlag.
- [3] Creager, M., and Paris, P. C., 1967, "Elastic field equations for blunt cracks with reference to stress corrosion cracking, " Int. J. Fract. Mech., **3**, pp. 247-252.
- [4] Savruk, M. P., and Kazberuk, A., 2006, "A relationship between the stress intensity and stress concentration factors for sharp and rounded notches," Mater. Sci., **42**, pp. 725-738.
- [5] Kim, J. K., and Cho, S. B., 2012, "A superposition approach to the stress fields for various blunt V-notches," Fatigue Fract. Eng. Mater. Struct., **36**, pp.139-153

- [6] Radaj, D., 2014, "State-of-the-art review on extended stress intensity factor concepts," *Fatigue Fract. Eng. Mater. Struct.*, **37**, pp. 1-28
- [7] Bahrami, B., Ayatollahi, M. R., and Mirzaei, A. M., 2019, "Analysis of stresses and displacements in the vicinity of blunt V-notches by considering higher order terms," *Fatigue Fract. Eng. Mater. Struct.*, **42**, pp. 1760-1774.
- [8] Kullmer, G., and Richard, H. A., 2006, "Influence of the root radius of crack-like notches on the fracture load of brittle components," *Arch. Appl. Mech.*, **76**, pp. 711-723.
- [9] Gómez, F. J., Elices, M., Berto, F., and Lazzarin, P., 2007, "Local strain energy to assess the static failure of U-notches in plates under mixed mode loading," *Int. J. Fract.*, **145**, pp. 29-45.
- [10] Livieri, P., and Segala, F., 2007, "Analytical evaluation of J-integral for elliptical and parabolic notches under mode I and mode II loading," *Int. J. Fract.*, **148**, pp. 57-71.
- [11] Zappalorto, M., and Lazzarin, P., 2014, "Some remarks on the Neuber rule applied to a control volume surrounding sharp and blunt notch tips," *Fatigue Fract. Eng. Mater. Struct.*, **37**, pp. 349-358.
- [12] Wang, X., and Schiavone, P., 2021, "Elastic field for a blunt crack represented by a parabolic cavity in a generally anisotropic elastic material," *Eng. Fract. Mech.*, **251**, pp. 107763.
- [13] Muskhelishvili, N.I., 1953, *Some basic problems of the mathematical theory of elasticity*. Noordhoff, Groningen.
- [14] Carpenter, W. C., 1984a, "Calculation of the fracture mechanics parameters for a general corner," *Int. J. Fract.*, **24**, pp. 45-58.

- [15]Carpenter, W. C., 1984b, “Mode I and Mode II stress intensities for plates with cracks of finite opening, ” Int. J. Fract., **26**, pp. 201-204.
- [16]Carpenter, W. C., 1994, “Comments on the eigenvalue formulation of problems with cracks, V-notched cracks, and corners,” Int. J. Fract., **68**, pp. 75-87.
- [17]Carpenter, W. C., 1995, “Insensitivity of the reciprocal work contour integral method to higher order eigenvectors,” Int. J. Fract., **73**, pp. 93-108.
- [18]Lazzarin, P., and Tovo, R., 1996, “A unified approach to the evaluation of linear elastic stress fields in the neighborhood of cracks and notches” Int. J. Fract., **78**, pp. 3-19.
- [19]Filippi, S., Lazzarin, P., and Tovo, R., 2002, “Developments of some explicit formulas useful to describe elastic stress fields ahead of notches in plates,” Int. J. Solids Struct., **39**, pp. 4543-4565.
- [20]Lazzarin, P., Zappalorto, M., and Berto, F., 2011, “Generalised stress intensity factors for rounded notches in plates under in-plane shear loading,” Int. J. Fract. , **170**, pp. 123-144
- [21]Mirzaei, A.M., Ayatollahi, M.R., Bahrami, B., and Berto, F., 2020, “Elastic stress analysis of blunt V-notches under mixed mode loading by considering higher order terms, ” Applied Mathematical Modelling, **78**, pp. 665-684.
- [22]Filon, L.N.G., 1900, “On the resistance to torsion of certain forms of shafting with special reference to the effect of keyways,” Philos. Trans. R. Soc. A, **193**, pp. 309-352.
- [23]Shepherd, W.M., 1932, “The torsion and flexure of shafting with keyways or cracks,” Proc. R. Soc. Lond. A, **138**, pp. 607-634.
- [24]Wigglesworth, L.A., 1939, “Flexure and torsion of an internally cracked shaft,” Proc. R. Soc. Lond. A, **170**, pp. 365-391.

- [25] Wigglesworth, L.A., and Stevenson, A.C., 1939, "Flexure and torsion of cylinders with cross-sections bounded by orthogonal circular arcs, " *Proc. R. Soc. Lond. A*, **184**, pp. 391-414.
- [26] Rushton, K.R., 1967, "Stress concentrations arising in the torsion of grooved shafts," *Int. J. Mech. Sci.*, **9**, pp. 697-705.
- [27] Ohr, S. M., Chang, S.J., and Thomson, R., 1985, "Elastic interaction of a wedge crack with a screw dislocation," *J. Appl. Phys.*, **57**, pp. 1839-1843.
- [28] Noda, N., and Takase, Y., 2003, "Generalized stress intensity factors for V-shaped notch in a round bar under torsion, tension and bending," *Eng. Fract. Mech.*, **70**, pp. 1447-1466.
- [29] Noda, N., and Takase, Y., 2006, "Stress concentration formula useful for all notch shape in a round bar (comparison between torsion, tension and bending)," *Int. J. Fatigue*, **28**, pp. 151-163.
- [30] Savruk, M.P., Kazberuk, A., and Tarasiuk, G., 2012, " Distribution of stresses over the contour of rounded V-shaped notch under antiplane deformation," *Mater. Sci.*, **47**, pp. 717-725.
- [31] Kim, J.-K., and Cho, S.-B., 2013, "Superposition approach of the stress fields for blunt V-notches under anti-plane shear loading," *International Journal of Precision Engineering and Manufacturing*, **14**, pp. 605-612.
- [32] Savruk, M. P., and Kazberuk, A., 2017, *Stress concentration at notches*, Springer.
- [33] Smith, E., 2004, "The elastic stress distribution near the root of an elliptically cylindrical notch subjected to mode III loadings," *Int. J. Eng. Sci.*, **42**, pp. 1831-1839.

- [34]Lazzarin, P., Zappalorto, M., and Yates, J.R., 2007, “Analytical study of stress distributions due to semi-elliptic notches in shafts under torsion loading,” *Int. J. Eng. Sci.*, **45**, pp. 308-328.
- [35]Zappalorto, M., Lazzarin, P., and Yates, J.R., 2008, “Elastic stress distributions for parabolic and parabolic notches in round shafts under torsion and uniform antiplane shear loadings,” *Int. J. Solids Struct.*, **45**, pp. 4879-4901.
- [36]Zappalorto, M., and Lazzarin, P., 2009, “A new version of the Neuber rule accounting for the influence of the notch opening angle for out-of-plane shear loads,” *Int. J. Solids Struct.*, **46**, pp. 1901-1910.
- [37]Salviato, M., and Zappalorto, M., 2016, “A unified solution approach for a large variety of antiplane shear and torsion notch problems: Theory and examples,” *Int. J. Solids Struct.*, **102-103**, pp. 10-20.
- [38]Ma, L.F., and Hills, D.A., 2022. “Interaction of a parabolic notch with a generalized singularity,” *Int. J. Eng. Sci.*, **176**, pp. 103685.
- [39]Ma, L.F., 2022, “Fundamental formulation for anti-plane eigenstrain problems,” *Mech. Mater.*, **165**, pp. 104188.
- [40]Rose, L.R.F., 1987, “The mechanics of transformation toughening,” *Proc. R. Soc. Lond. A*, **412**, pp. 169-197.
- [41]Ma, L.F., 2010, “Fundamental formulation for transformation toughening,” *Int. J. Solids Struct.*, **47**, pp. 3214-3220.
- [42]Wang, X., and Schiavone, P., 2021, “A screw dislocation located outside, inside or on the interface of a parabolic elastic inhomogeneity,” *Arch. Mech.*, **73**, pp. 219-235.
- [43]Eshelby, J.D., 1951, “The force on an elastic singularity,” *Philosophical Transactions of the Royal Society of London A*, **244**, pp. 87-112.

- [44]Cherepanov, G.P., 1967, “The propagation of cracks in a continuous medium,”
Journal of Applied Mathematics and Mechanics, **31**, pp. 503-512.
- [45]Rice, J.R., 1968, “A path independent integral and the approximate analysis of
strain concentration by notches and cracks,” J. Appl. Mech., **35**, pp. 379-386.
- [46]Budiansky, B., and Rice, J.R., 1973, “Conservation laws and energy-release
rates,” J. Appl. Mech., **40**, pp. 201-203.
- [47]Hills, D. A., Kelly, P. A., Dai, D. N., and Korsunsky, A. M., 1996, Solution of
Crack Problems: The Distributed Dislocation Technique, Kluwer Academic
Publishers, Dordrecht, the Netherlands.